Assessment of high-enthalpy composite eutectic phase change materials efficiency in asphalt binders for cooling pavements

Published Version:
Dai, J., Feng, M.a., Sangiorgi, C., Tarsi, G., Zhen, F.u., Tataranni, P., et al. (2024). Assessment of high-enthalpy composite eutectic phase change materials efficiency in asphalt binders for cooling pavements. JOURNAL OF CLEANER PRODUCTION, 442, 1-14 [10.1016/j.jclepro.2024.140999].

Availability:
This version is available at: https://hdl.handle.net/11585/956413 since: 2024-02-09

Published:
DOI: http://doi.org/10.1016/j.jclepro.2024.140999

Assessment of high-enthalpy composite eutectic phase change materials efficiency in asphalt binders for cooling pavements

Jiasheng Dai [a, b], Feng Ma [a, *], Cesare Sangiorgi [b], Giulia Tarsi [b], Zhen Fu [c], Piergiorgio Tataranni [b], Chen Li [a], Yingjie Hou [a]

[a] Key Laboratory for Special Area Highway Engineering of Ministry of Education, Chang'an University, Xi'an, Shaanxi, 710064, China

[b] Department of Civil, Chemical, Environmental and Materials Engineering, University of Bologna, Bologna, 40131, Italy

[c] School of Material and Science Engineering, Chang'an University, Xi'an, Shaanxi, 710064, China

*Correspondence: mafeng@chd.edu.cn

Abstract: Phase change materials (PCMs) as thermal energy storage solutions can mitigate pavement damage and alleviate the urban heat island effect. A stable shape, suitable melting temperature, and high-enthalpy can extend the application potential of PCMs in cooling pavements. The goal behind this study is to investigate the potential use of two high-enthalpy composite phase change materials (CPCMs) in an SBS-modified asphalt binder through thermal and chemo-rheological tests. Herein, using a ternary eutectic mixture with adipic/sebacic/stearic acids (named A) and a binary eutectic mixture consisting of stearic/palmitic acids (named B) as two distinct PCMs and expanded graphite as supporting material, two novel CPCMs were successfully prepared through vacuum impregnation. The findings showed that the encapsulation efficiency of both CPCM-A and CPCM-B exceeded 90%. The melting enthalpy (H_m) and the melting phase-change temperatures (T_m) values were 193.3 J/g and 61.7°C for CPCM-A, 189.6 J/g, and 50.5°C for CPCM-B. The H_m of the two related asphalt binders that incorporate the developed CPCMs (SBS-A and

SBS-B) were 19.5 J/g and 17.2 J/g, respectively, indicating high thermal storage and management capabilities. This allowed SBS-A and SBS-B to exhibit maximum temperature differences of 13.1°C and 10.7°C, with temperature lags of 1500 s and 2610 s, respectively. Also, the CPCMs and the related asphalt binders presented outstanding thermal and chemical stability. The CPCMs enhanced the resistance to deformation and deformation recovery capability of asphalt at high temperatures and under severe loads. However, SBS-B experienced an earlier phase transition than SBS-A, ultimately leading to a diminished ability to withstand deformation at the testing temperature. To sum up, opting for CPCM-A over CPCM-B for asphalt pavement cooling applications is advisable.

Keywords: Cooling pavements; composite phase change materials; asphalt binders; thermal-regulating properties; rheological characterization

Graphical Abstract:

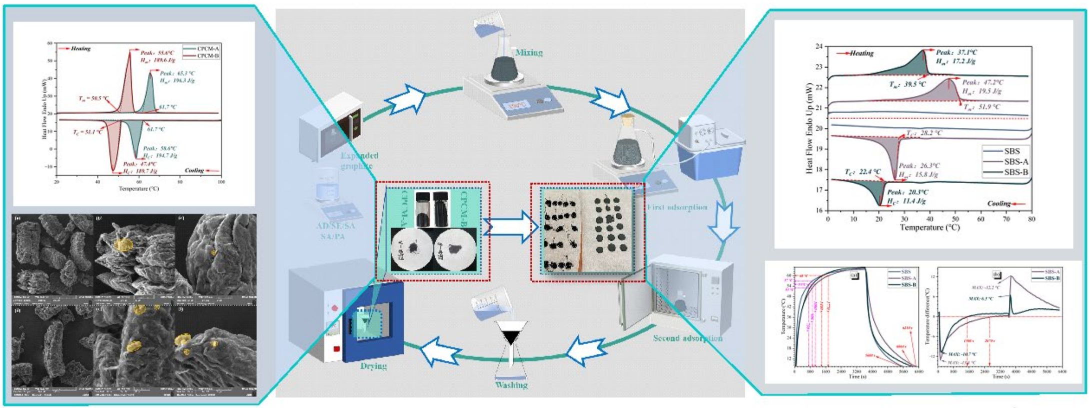

1. Introduction

The urbanization process has caused the emergence of the urban heat island (UHI) effect, whereby urban areas are generally warmer than the surrounding rural environment, especially during summer (Anupam et al., 2023). This phenomenon is attributed to several factors, including the use of certain building materials, the complex geometry of urban landscapes, reduced vegetation cover, and increased anthropogenic heat emissions (Nwakaire et al., 2020). Among all factors, the low reflectivity of black asphalt pavements is one of the leading contributors to the UHI effect, as it absorbs a significant proportion of solar radiation, which turns into high pavement-surface temperatures up to 60°C during summer (Wang, C. et al., 2021). The UHI poses considerable health risks to urban residents, including heat-related illnesses and fatalities (Anderson and Bell, 2011). Additionally, asphalt pavements' viscoelastic and temperature-susceptible properties make them prone to several damages when exposed to prolonged high temperatures (Chen et al., 2020). These damages include rutting and thermo-oxidative aging, which eventually affect the durability and serviceability of road pavements (Yuan et al., 2023a).

To ensure that cities are livable with enhanced environmental quality and sustainable energy consumption patterns, it is imperative to adopt UHI mitigation strategies to address these pavement-related adverse consequences, such as installing reflecting and permeable pavements (Gong et al., 2023; Zhang, D.R. et al., 2023). However, such strategies may affect pedestrians’ thermal comfort, increasing building energy consumption and carbon emissions (Li et al., 2013). Pavement design that integrates renewable energy technologies, such as latent heat structures and photovoltaic materials, has emerged as a promising approach to mitigate UHI (Guo et al., 2020; Yuan et al., 2023b). These systems achieve surface temperature reduction by converting absorbed radiation into different kinds of energy.

A different solution for mitigating the UHI is represented by phase change materials (PCMs). The PCMs are functional materials that have the innate capability to absorb and release thermal energy during their phase transition, offering a potential mechanism for the regulation of temperature variances within pavement structures (Ye et al., 2014). Such thermoregulatory attributes can extend the longevity of road pavements by mitigating the frequency of thermally induced mechanical stresses (Zhang, J. et al., 2023). Concurrently, when integrated into pavement systems, the PCMs can incorporate superfluous thermal energy at maximal temperatures achieved during the daytime, resulting in a marked reduction of the pavement's surface temperature (Wu et al., 2022). Subsequently, as temperatures decrease, particularly during cooler periods like nighttime, phase change materials (PCMs) progressively discharge the accumulated thermal energy. Although this released heat energy leads to an elevation in pavement temperature, the gradual discharge of heat aids in regulating ambient temperatures, leading to a more consistent thermal environment in comparison to the rapid heat release from conventional surfaces (Roman et al., 2016; Salem and Bichara, 2023). Their application in urban structures also helps mitigate the UHI by moderating surface temperatures and minimizing temperature fluctuations within urban environments., presenting a viable strategy to counteract the UHI (Kakar et al., 2019b; Tyagi et al., 2021).

Therefore, it may be feasible to depend on the phase-change thermal characteristics of PCMs to endow the pavement with latent heat ability, thereby alleviating the temperature stress and UHI. Zhang et al. (Zhang, J. et al., 2023) incorporated 4% paraffin/expanded graphite/high-density polyethylene composites into asphalt binder, showing a temperature difference of 4°C and a delay time of 456 s. Polyurethane solid-solid PCMs were synthesized by Jia et al. (Jia et al., 2023), Liu et al. (Liu et al., 2023), and Jiao et al. (Jiao et al., 2023) to equip asphalt binder with thermal regulation properties and decrease the temperature of road pavements. According to previous reteaches, the integration of expanded graphite (EG)/polyethylene glycol (PEG) as composite phase change materials (CPCMs) into asphalt binders resulted in enhanced resistance to rutting and noticeable cooling effect (Zhang, D. et al., 2018; Zhang et al., 2019). Meanwhile, Jin et al. (Jin et al., 2021; Jin et al., 2018) utilized diatomite and stearic acid (SA) to develop excellent chemical and thermal stability CPCMs. This innovative approach decreased the temperature of the upper and lower surfaces of asphalt pavement by 10.90°C and 5.03°C, respectively. Farnam et al. (Farnam et al., 2016) integrated lightweight aggregates with PCM into the pavement, resulting in a significant maximum heat release potential of 12.11 kJ/m^3. Furthermore, Dai et al. (Dai et al., 2021; Dai et al., 2022), Jia et al. (Jia et al., 2021), Du et al. (Du et al., 2019), and Kakar et al. (Kakar et al., 2019a) reported that the direct introduction of PCM would soften the asphalt binder due to the liquefaction after the phase transition of PCM, resulting in a significant decrease in both its viscosity and elasticity. Obviously, the previous research presented a viable approach for utilizing PCM for pavement cooling. Nevertheless, some obstacles might significantly constrain its widespread implementation, such as unreasonable encapsulation strategies, mismatched melting temperature, low-enthalpy, etc. Further studies on the utilization of PCMs in cooling pavements mainly revolve around two subjects: the selection of PCM and the encapsulation technology. Table 1 compiles the findings of investigations on using CPCMs in cooling pavements. It can be concluded that the methods of CPCMs preparation primarily include chemical synthesis, microencapsulation, and vacuum adsorption, with an enthalpy of below 100 J/g. Moreover, the selection of PCM mainly focuses on PEG, SA, and paraffin. However, phase change temperature and enthalpy are two inherent features of PCM (Hasanabadi et al., 2021). It is challenging to find naturally occurring solid-liquid PCMs that meet both a reasonable phase change temperature and a high enthalpy (Bai et al., 2018). Therefore, developing an ideal CPCM with the maximum possible enthalpy, appropriate phase change temperature, and stable packaging technology is imperative.

Table 1 Summary of preliminary research on the application of CPCMs in cooling pavements

PCMs	Supporting materials	Encapsulation Technology	Phase change temperature (°C)	Phase change enthalpy (J/g)	Ref.
PEG-800	Polyacrylamide	Graft copolymerization	17.10	72.2	(Cheng et al., 2021)
PEG-1000	Diatomite	Vacuum adsorption	40.12	67.48	(Wang, H. et al., 2021)
PEG-2000	Lightweight aggregate	Vacuum adsorption	53.00	7.96-17.69	(Yinfei et al., 2020)
PEG-2000	Cement	Polymeric hydration	53.59	37.47	(Du, Y. et al., 2021)
PEG-2000	Hydrophobic fumed silica	Sol-gel	50.00	173.60	(Hu et al., 2021)
PEG-2000	Expanded graphite	Vacuum adsorption	45.33-50.07	120.45-137.94	(Zhang, D. et al., 2018)
PEG-4000	Silica	Sol-gel	62.80	48.50	(Chen et al., 2019)
PEG-4000	-	Chemical bonding	25.60-45.70	58.60-128.40	(Liu et al., 2023)
PEG-8000	-	Chemical bonding	50.20	115.20	(Jia et al., 2023)
Paraffin	Expanded perlite	Vacuum adsorption	62.30	76	(Hasanabadi et al., 2021)
Paraffin	high-density polyethylene	--	11.00-37.00	186.00	(Zhang, J. et al., 2023)
Paraffin	Polyurethane/epoxy resin	One-step	-0.33	14.40	(Bai et al., 2018)
SA	Montmorillonite	-	40.00-85.00	221.60	(Liu et al., 2022)
SA	Mineral-supported	Vacuum adsorption	66.77-67.13	105.50-143.7	(Jin et al., 2021)
Pentadecane	Nano-silica and ethyl cellulose	Microencapsulation	15.30	117.40	(Ma et al., 2019)

On top of that, the use of eutectic technique for PCMs is a compelling advancement in the ongoing researches, as it enables customization of the melting point to meet specific requirements (Du, W. et al., 2021). The eutectic technique involves blending two or more fatty acids in a particular mass proportion to achieve the least possible melting point, which considerably simplifies the task of matching PCMs while expanding their higher latent heat (Yang et al., 2019). A set of multiple eutectic mixes based on fatty acids with 10-18 carbons was described by Ke et al. (Ke, 2017) and Nazir et al. (Nazir et al., 2018), with phase change temperatures between 15°C and 50°C. Furthermore, some naturally dicarboxylic acids (DA), such as adipic acid (AD) and sebacic acid (SE), possess the advantages of being cost-effective, abundantly available, and having a high enthalpy. However, their usage is limited due to their high melting point (AD-152.1°C, SE-134.5°C) (Haillot et al., 2011; Kolyado et al., 2016). Eutectic technology can incorporate these DA into asphalt pavements. Ma et al. (Ma et al., 2018) reported the thermal properties and stability of three binary eutectic mixtures of AD/SA, SE/SA, and suberic acid/SA binary eutectic PCMs, with the following melting temperatures: 67.45°C, 66.37°C, and 67.08°C. Seki et al. (Seki et al., 2015) employed graphite nanosheets to load an AD/SE eutectic mixture, achieving a melting temperature of 116°C. Nevertheless, literature is lacking concerning using DA in cooling pavements. Moreover, EG is a novel carbon-based material with impressive attributes such as exceptional thermal conductivity, absorption capacity, thermal stability, and compatibility (Zhang, D. et al., 2018). The EG can serve as a PCM-supporting material to mitigate the leakage of PCM itself and enhance heat transfer efficacy. Hence, exploiting the positive experience of eutectic PCM in thermal energy storage is a forward-thinking approach to developing an asphalt pavement with temperature-regulating capability.

In the present study, two high-enthalpy CPCMs were developed employing vacuum impregnation, using AD/SE/SA and SA/PA eutectic mixtures as phase change units and EG as supporting material. Notably, AD and SE were first introduced into asphalt pavements as energy storage materials. Initially, the phase change behavior, and thermal and chemical stability of the two CPCMs were assessed. Then, the CPCMs were integrated into the SBS-modified asphalt binder, and the resulting binders underwent thermal and chemo-rheological characterizations.

2. Materials and test methods

2.1 Raw Materials

2.1.1 Asphalt binder

Styrene-butadiene-styrene (SBS) polymer-modified asphalt, graded as 40/100-55, produced by an Italian company, was used as a base and control binder in this research. The conventional physical properties of the soft modified asphalt binder provided by the supplier are listed in Table 2.

Table 2 Physical properties of SBS-modified bitumen 40/100-55 (from the technical data sheet)

Characteristics	**Property**	**Method**	**Unit**	**Performance**	
				min	**max**
Consistency at intermediate service temperatures	Penetration at 25°C	EN 1426	dmm	45	70
Consistency at high service temperatures	Softening Point P.A.	EN 1427	°C	55	
Cohesion	Force Ductility Test at 5°C	EN 13589 EN 13703	J/cm^2	3.0	
Durability Resistance to RTFOT aging	Mass variation	-	%		0.8
	Residual penetration at 25°C	EN 1426	%	50	
	Δ Softening point	EN 1427	°C		10
Flammability	Flash point	EN ISO 2592	°C	250	
Dynamic viscosity	Viscosity at 160°C	EN 13302	Pa.s	0.30	
Deformation recovery	Elastic Return at 25°C	EN 13398	%	60	
Storage stability/EN13399	Δ Softening point	EN 1427	°C		5
	Δ Penetration at 25°C	EN 1426	dmm		9

2.1.2 Fatty acids

Four fatty acids were selected as PCMs provided by Shanghai Macklin Biochemical Technology Co., Ltd, including palmitic acid (PA), stearic acid (SA), sebacic acid (SE), and adipic acid (Ad). Some of their information is listed in Table 3. The supplier furnished the essential data, while a differential scanning calorimeter (DSC) determined the phase change temperature and enthalpy.

The abovementioned materials were combined to produce two high-enthalpy PCMs. One ternary and one binary eutectic mixture were developed as phase change units: AD/SE/SA and SA/PA. The two PCMs are coded as A and B, respectively.

Table 3 Information on fatty acids

Item	CAS No	Linear Formula	Molecular Weight	Purity (%)	Phase-change temperature (melting, ℃)	Phase-change enthalpy (melting, ℃)
PA	57-10-3	$CH_3(CH_2)_{14}COOH$	256.42	99	61.10	213.29
SA	57-11-4	$CH_3(CH_2)_{16}COOH$	284.48	98	67.70	223.75
SE	124-04-9	$HOOC(CH_2)_4COOH$	146.14	≥98	151 - 154	267.55
AD	111-20-6	$HOOC(CH_2)_8COOH$	202.25	99	133 - 137	247.83

2.1.3 Expanded graphite

Expanded graphite (EG) was used as a supporting material for the two PCMs. The used expanded graphite has a particle size of 80 mesh, an expansion rate of 200 to 350 times, and a purity level of 99%.

2.2 Determination of the mass proportion of binary/ternary eutectic phase change materials (PCMs)

The theoretical molar ratio of a mixture was determined using the Schrader Equations (1 and 2), derived from the second law of thermodynamics and phase equilibrium theory (Kolyado et al., 2016). Then, the theoretical molar ratios of the SA/PA binary eutectic mixture and AD/SE/SA ternary mixture were translated to theoretical mass ratios (Ke, 2017; Nazir et al., 2018). When calculating the eutectic point for a ternary mixture, the AD/SE binary mixture was treated as a new single pure component, and a third phase (SA) was introduced to form AD/SE/SA ternary eutectic mixture.

$$\ln X_i = \frac{\Delta H_i}{R}\left(\frac{1}{T_i} - \frac{1}{T}\right) \ (i = A, B) \quad (1)$$

$$X_A + X_B = 1 \quad (2)$$

Where, X_i is the mole percentage of component i, T_i is the melting temperature of component i(K)，R is the gas constant (8.314 J/(mol·K)，and ΔH_i is the molar heat of fusion of component i (J/mol).

Based on this, the mass ratios of the AD/SE/SA ternary mixture and SA/PA binary eutectic mixture were 0.0305:0.0658:0.9037 and 0.398:0.602, respectively.

2.3 Preparation of samples

2.3.1 Preparation of composite phase change materials (CPCMs)

The melt blending method was used to prepare eutectic mixtures of the two PCMs. The appropriate mass of all fatty acids was placed on an analytical scale with an accuracy of 0.001g, and then, the composite materials were put into a preheated oven at 150°C. When the samples were melted, they were put in a magnetic stirrer and mixed at 300 rpm for 2 h at 100°C to obtain the corresponding binary/ternary eutectic mixture.

The CPCMs were synthesized using a vacuum impregnation technique, with the eutectic mixture as the core material and the EG as the supporting one. This involved drying a certain quantity of EG in an oven at 100°C for 24 h to eliminate moisture and rotating it in a microwave oven for two minutes to obtain fully EG. Once ready, the EG was mixed with one of the melted eutectic mixtures in a suction flask, considering a mass ratio of 1:15 (PCM:EG). Then, the suction filter flask was placed on a magnetic stirrer at a temperature of 85°C at 100 rpm and evacuated with a vacuum pump at 0.12 MPa for 4 h to facilitate the impregnation of the eutectic mixture into the pore structure of EG. After this mixing phase, the suction flask was placed in a vacuum oven at 85°C for 48 h to ensure the full impregnation of EG with the eutectic mixture. The obtained black mixture was subsequently washed four times with absolute ethanol. Finally, the rinsed sample was placed in an oven at 60°C for 4 h to evaporate absolute ethanol completely. The final dry product obtained is the CPCM, and the detailed synthesis process of CPCM is presented in Figure 1. The same procedure was replicated to produce both CPCMs. The two CPCMs produced with the ternary and binary eutectic mixtures are indicated as CPCM-A and CPCM-B, respectively.

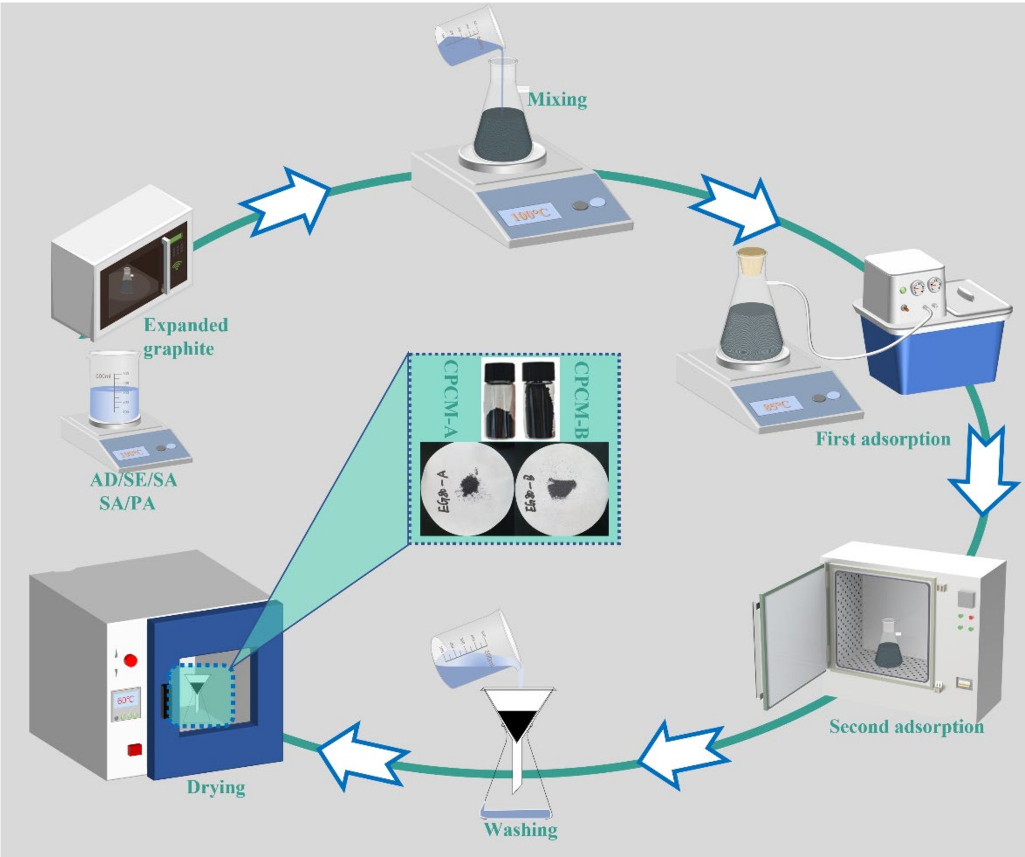

Figure 1 The detailed synthesis process of CPCMs

2.3.2 Preparation of composite phase change asphalt binders

A propeller mixer was used to manufacture the SBS-modified asphalt binders incorporating the two CPCMs. Since 15% SA/PA content had been shown to have little effect on the asphalt binder while exhibiting outstanding temperature regulation performance in our earlier research (Dai et al., 2021; Dai et al., 2022; Dai et al., 2023), both samples were added at that concentration (by mass of original SBS-modified asphalt binder). Following, the CPCMs and the preliminary heated asphalt binder were mixed at 140°C at a mixing rate of 1000 rpm for 30 minutes.

2.4 Thermal, chemical, and rheological characterizations

2.4.1 Differential scanning calorimeter tests

The heat storage and release capabilities of two CPCMs and three asphalt binders (i.e., SBS, SBS-A, and SBS-B) were assessed using a differential scanning calorimeter (DSC, DSC 4000, PerkinElmer). The DSC tests were operated at a heating/cooling rate of 5°C/min in a nitrogen atmosphere while each sample underwent two heating-cooling cycles within the temperature range between 0°C and 100°C. A five-minute equilibration period was implemented after each heating/cooling cycle to eliminate any thermal history and reduce measurement errors. Four key thermal parameters, including the variation of melting enthalpy (ΔH_m), melting phase transition temperature (T_m), the variation of cooling enthalpy (ΔH_c), and cooling phase transition temperature (T_c), were defined to provide a clearer description of the sample's phase transition process. For further details, please refer to Figure 2.

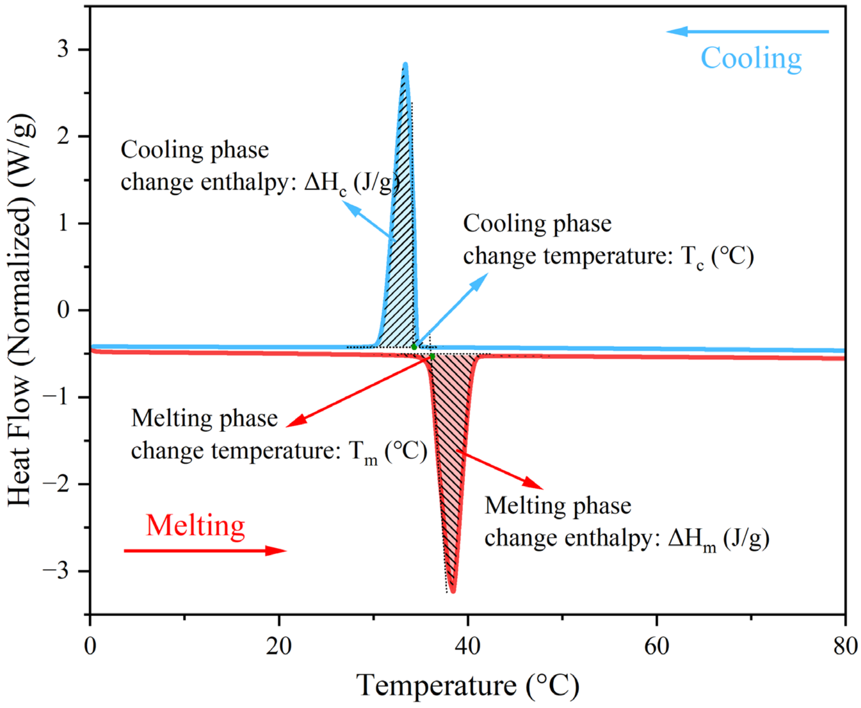

Figure 2 Determination of the phase-change parameters

2.4.2 Attenuated Total Reflection Fourier Transform Infrared tests

The chemical structure of the two CPCMs and the three asphalt binders was analyzed using the Fourier Transform Infrared Spectrometer (FTIR, Spectrum 3, PerkinElmer) in the attenuated total reflectance (ATR) mode. Measurements were taken in wavelengths from 500 to 4000 cm^{-1} to capture the spectra, performing 32 scans at 4 cm^{-1} for each sample. Two replicates of each sample were carried out.

2.4.3 Thermogravimetric tests

To ensure the temperature regulation ability of CPCMs in cooling asphalt pavement, they must be endowed with superior thermal stability, which turns into thermal durability in the corresponding working setting. The thermogravimetric analysis instrument (TGA, TGA 4000, PerkinElmer) was used to characterize the thermal stability of the three asphalt binders and the two CPCMs. The experiment was conducted under a nitrogen atmosphere, whereby approximately 20 mg of the sample was heated at a rate of 10°C/min from 30°C to 600°C. The test was replicated two times per specimen.

2.4.4 Microstructure analysis

Scanning electron microscopy (SEM, MIRA3 TESCAN, Czech Republic) was employed to obtain CPCM-A and CPCM-B microstructure images. To prevent the occurrence of blurry images caused by the low electronic conductivity of the specimens, the CPCMs that were uniformly distributed on the supporting tools underwent metallization treatment using gold (Lecia EM ACE600). The images were captured at an accelerating voltage of 15 kV.

2.4.5 Rheological tests

The dynamic shear rheometer (DSR, MCR 302, Anton Paar, Austria) was utilized to measure the rheological properties of the asphalt binders. It is common practice to use the DSR to characterize asphalt's viscoelastic properties by measuring several rheological parameters, including complex shear modulus (G^*) and phase angle (δ), of tests run under controlled temperature, loading frequency, and strain magnitude conditions. Samples' preparation and testing apparatus followed the EN 14770 standard using the 25-mm parallel plate geometry with a 1-mm gap setting (ASTM, 2015).

Preliminarily, the amplitude sweep tests were carried out to define the linear viscoelastic (LVE) range of the asphalt binders at three test temperatures, 20°C, 40°C, and 70°C, and the results are shown in Figure 3. The test temperatures were selected to cover the temperature range between 20°C and 70°C at which the temperature sweep tests were performed. The corresponding strain at 95% of the initial storage modulus (the elastic component of G^*) has been selected to mark the threshold of non-destructive deformation, i.e., the LVE range. Therefore, to guarantee that the three asphalt binders remained within the LVE range during the temperature sweep tests, a strain of 0.1% was selected. As anticipated, during the temperature sweep tests, the temperature varied between 20°C to 70°C at a rate of 2°C/min, while the frequency was maintained at a constant value of 10 rad/s.

The Multiple Stress Creep and Recovery (MSCR) test followed the ASTM D7405-15 standard. The sample was loaded at a constant stress for 1 s and then allowed to recover for 9 s. Twenty creep and recovery cycles were run at 0.1 kPa, followed by ten creep and recovery cycles at 3.2 kPa. The MSCR tests were conducted at four distinct temperatures (precisely 30°C, 40°C, 50°C, and 60°C) to investigate the phase-change behavior of CPCMs comprehensively. Finally, the data were extracted to calculate the creep parameters: average percent recovery at 0.1 kPa ($R_{0.1}$) and 3.2 kPa ($R_{3.2}$) and the average non-recoverable creep compliance at 0.1 kPa ($J_{nr0.1}$) and 3.2 kPa ($J_{nr3.2}$), according to ASTM D7405-2015. The two parameters at the lowest creep load only considered the latest 10 cycles. Two replicates were performed in the temperature sweeps and MSCR tests. The rheological tests were replicated two times per specimen.

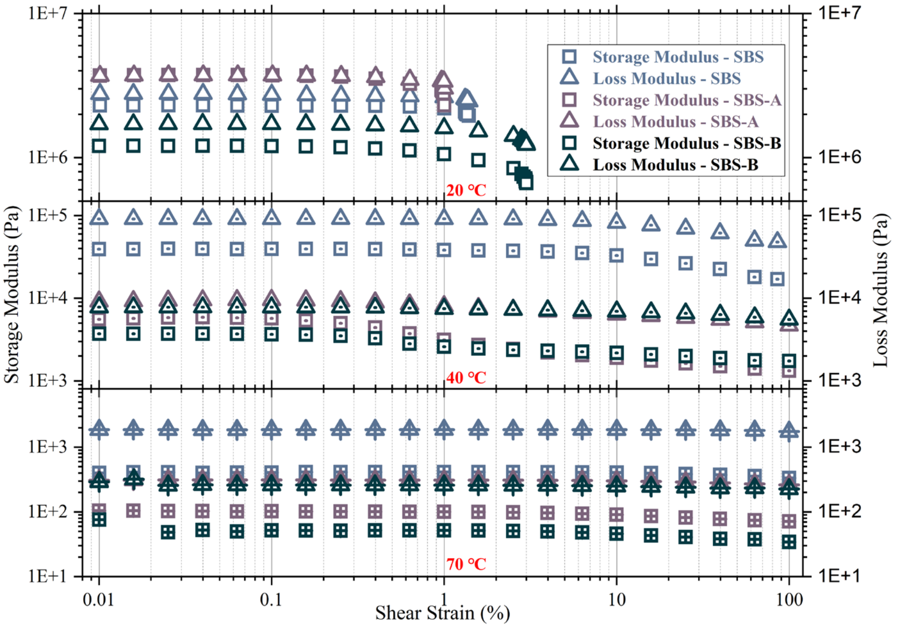

Figure 3 The linear amplitude sweeps of asphalt binders

2.4.6 Temperature-time curve tests

To assess the thermal regulation capabilities of the three types of asphalt binders, temperature-time curves were continuously monitored while subjecting the samples to a consistent temperature of 65°C. Initially, 50 g of the sample was weighed and transferred to a beaker, which was then stored in a refrigerator at 4°C for 2 h to ensure that all samples were conditioned at the same initial test temperature. The samples were subsequently placed in an oven and heated until the temperature stabilized at 65°C. At that point, they were removed and returned to the refrigerator to monitor the cooling process. The asphalt binders setting and the temperature acquisition instrument are presented in Figure 4. Two replicates were taken.

Figure 4 Schematic diagram of temperature acquisition

3. Results and discussion

3.1 Thermal properties of CPCMs

3.1.1 Phase change behaviors of CPCMs

The phase-change enthalpy represents a significant parameter when assessing the thermal energy storage potential of a PCM, while the phase-change temperature determines its suitable operational environment (Dai et al., 2023; Hou et al., 2023; Jia et al., 2022). As shown in Figure 5, the heat flow curves of both CPCMs exhibited apparent endothermic and exothermic peaks during the melting and cooling processes, suggesting that the PCMs were effectively encapsulated in EG. The thermal regulation properties of a material are generally enhanced with higher enthalpy values (Wei et al., 2022). The CPCM-A and CPCM-B showcased significant melting enthalpies of 193.3 J/g and 189.6 J/g, respectively. Given that the support material, EG, lacks latent heat properties, it was evident that these enthalpies originated from AD/SE/SA and SA/PA. Therefore, the encapsulation efficiency (η), calculated by dividing the melting enthalpy of CPCMs by the melting enthalpy of eutectic PCMs, was derived inversely. With the original melting enthalpies for these eutectic PCMs approximated at 211 J/g, encapsulation efficiencies exceeded 90%. Notably, the phase-change temperatures (T_m) of CPCM-A and CPCM-B were recorded at 61.7°C and 50.5°C, respectively. Minor reductions in T_m, 2.14°C for CPCM-A and 2.32°C for CPCM-B, may be attributed to the EG's porous cross-linked network impeding eutectic PCM molecular movements (Ma et al., 2023). Meanwhile, the melting and cooling stages of the two kinds of CPCMs exhibited symmetric melting and cooling peaks with no discernible supercooling effect. The supercooling degrees of CPCM-A and CPCM-B were determined to be 0°C and 0.6°C, respectively, indicating outstanding crystallization properties. The CPCMs had appropriate crystallization temperatures of 61.7°C and 51.1°C, ensuring their resilience to thermal cycling in asphalt pavement environments.

Compared with Table 1, the enthalpy of CPCMs in this work is around 2÷3 times greater than most of previous studies on this topic (Chen et al., 2019; Liu et al., 2023; Ma et al., 2019; Wang, H. et al., 2021). These findings highlighted the CPCMs' superior temperature regulation capabilities, making them prime candidates for enhancing asphalt pavement performances.

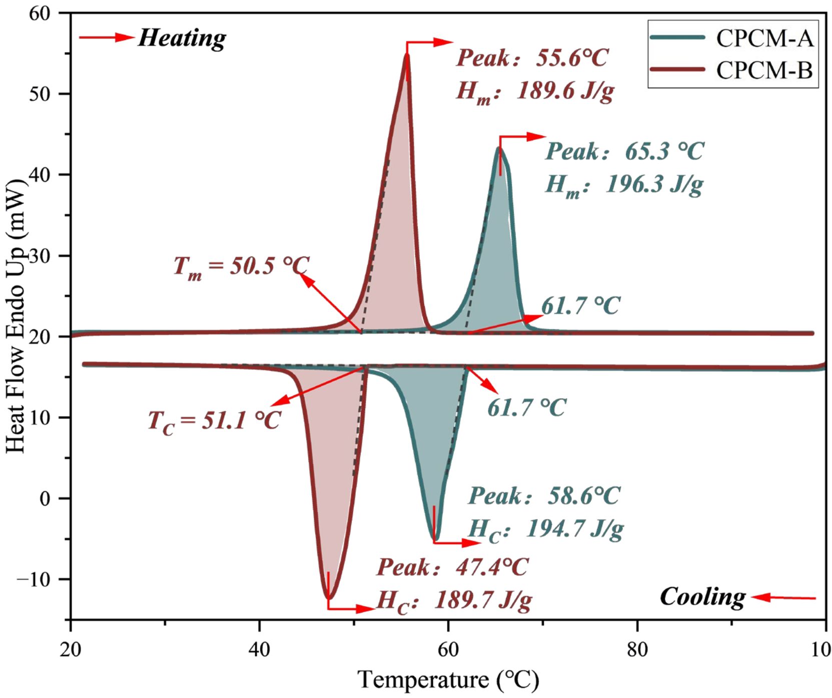

Figure 5 The heat flow curves of CPCMs obtained from DSC tests

3.1.2 Thermal stability of CPCMs

The thermal decomposition curves of CPCMs with increasing temperature and their corresponding derivative weight curves are shown in Figure 6. Given that standard operational conditions of asphalt pavements do not exceed 70°C, the crucial threshold temperature of a hot mix asphalt mixtures lies at 180°C (marked by the red line in Figure 6) (Dai et al., 2021). Both CPCM-A and CPCM-B exhibited remarkable thermal stability within the working temperature. Specifically, these CPCMs displayed a mass retention of 100% at 180°C. This indicates their resistance to thermal decomposition at typical mixing temperatures of hot asphalt mixes. Moreover, the onset and completion temperatures for thermal decomposition of the CPCMs were observed at 190°C and 350°C, respectively, with the highest decomposition rates detected at 291°C for CPCM-A and 303°C for CPCM-B. Based on these results, it is reasonable to conclude that CPCM-A and CPCM-B have the required thermal stability to meet the demands of the asphalt pavement industry throughout the construction and service stage (Zhang, J. et al., 2023). It is noteworthy that EG exhibited great stability up to 400°C without undergoing any thermal reactions, ensuring a constant quality of the material (Zhang et al., 2021; Zhang, D. et al., 2018). As a result, the weight loss during the thermal decomposition reaction is solely attributed to the eutectic PCMs. This phenomenon is reflected by the peak areas in the derivative weight curve, revealing that CPCM-A and CPCM-B exhibited peak areas of 90.0% and 91.8%, respectively. This reinforces that EG's encapsulation efficiency of eutectic PCMs exceeded 90%.

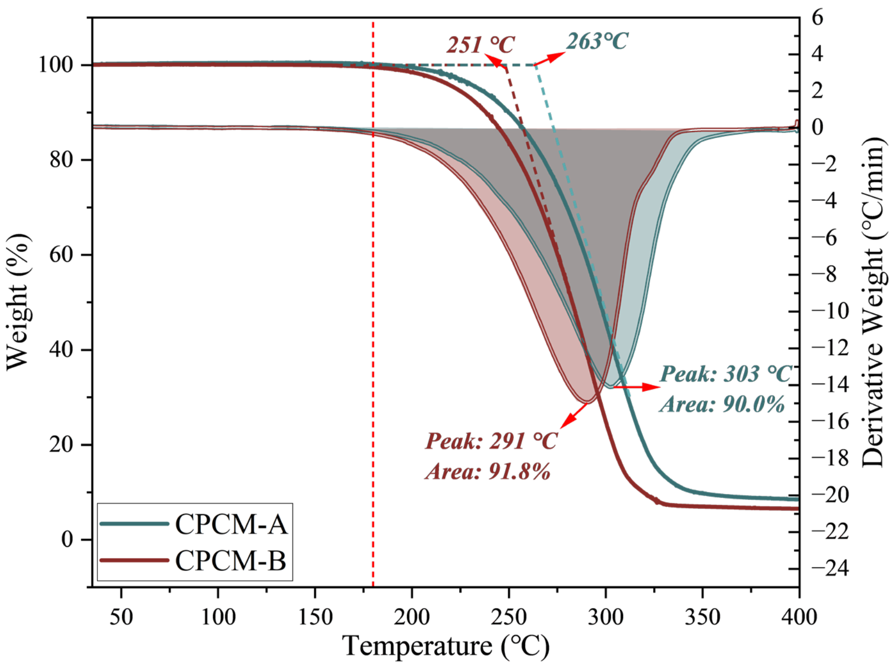

Figure 6 The TG and DTG curves of CPCMs

3.2 Microstructure analysis of CPCMs

Figure 7 displays the SEM images of CPCMs at different magnifications. According to the previous findings (Li et al., 2019; Liu et al., 2014; Zhang, D. et al., 2018), EG with a highly porous structure enhances its ability to adsorb liquefied PCMs. This porous quality is pivotal in applications where high adsorption is desired. From the images, specifically Figures 7 (a) and (d), the worm-like or layered configuration without discernible pore structures of CPCMs powders was visible. This specific structural configuration suggested a heightened capability of eutectic PCMs to permeate these structures under a vacuum, hence filling the available voids. This results in a remarkable adsorption capacity, reaching up to 90% for eutectic PCMs. Additionally, the dissolution and washing process using absolute ethanol effectively removed many eutectic PCMs remaining on the external surface of EG particles. This prevents the leakage of eutectic PCMs when EG is subjected to capillary force and surface tension after melting, thereby behaving as solid-solid PCMs on a macroscopic scale. However, as marked by yellow areas in Figures 7 (b), (c), (e), and (f), there were small proportions of unencapsulated or free-eutectic PCMs on EG surfaces. While this fraction is minor, its melting can cause infiltration into the asphalt binder. Even though the impact of this infiltration might be perceived as marginal in the context of asphalt pavement performance, especially in severe environmental conditions, even slight alterations in binder properties may have adverse and cumulative effects over time. This observation might pave the way for future research to optimize the encapsulation process, thus enhancing the long-term performance and durability of the asphalt pavements integrated with these PCMs.

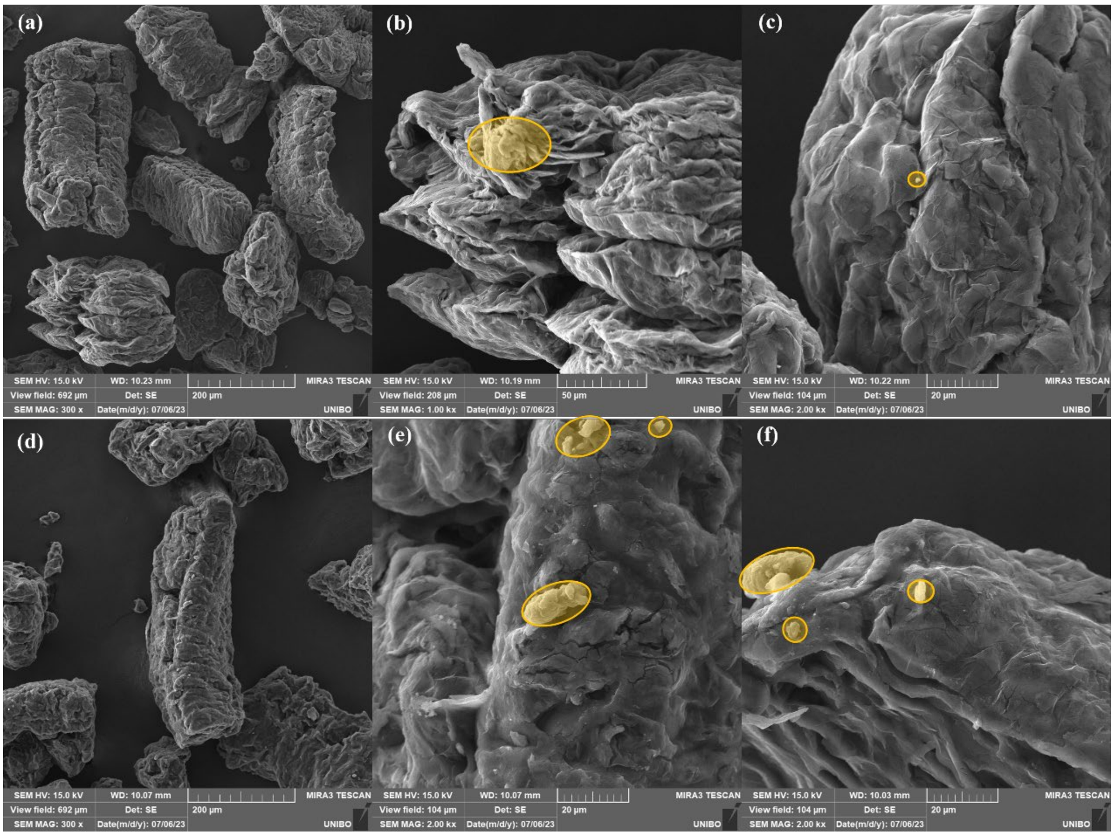

Figure 7 SEM images of CPCMs: (a), (b), and (c) CPCM-A; (d), (e), and (f) CPCM-B

3.3 Chemical stability of CPCMs and modified asphalt binders

3.3.1 FTIR results of CPCMs

The FTIR proves to be a highly efficient instrument for investigating the chemical structure of materials in terms of functional groups. The FTIR spectra of CPCMs and asphalt binders are shown in Figures 8 and 9, respectively. The spectra of CPCM-A and CPCM-B exhibited characteristic peaks of comparable intensity, indicating their similarity in terms of chemical structure. Strong peaks were observed at 2913 cm^{-1}, 2848 cm^{-1}, and 1700 cm^{-1}, primarily attributing to the alkali CH_2 anti-stretching, CH_3 symmetrical stretching, and carboxylic acid carbonyl C=O stretching. The medium-intensity peaks at 1470 cm^{-1} and 1430 cm^{-1} corresponded to the variable angle of the alkane CH_2 and the in-plane bending carboxylic acid COH, respectively. Additionally, CH_3 symmetrical stretching contributed to the appearance of a weak peak at 2955 cm^{-1}. The fingerprint region of the spectrum, ranging from 1330 cm^{-1} to 400 cm^{-1}, was also analyzed. The vibration of the fingerprint region can be attributed to the vibration of the whole molecule or a portion of the molecule and not the vibration frequency of a specific group. The peaks at 1300-1200 cm^{-1} and 950-900 cm^{-1} aligned with the stretching and out-of-plane bending of carboxylic acid C-OH. Moreover, the C-C extension of the straight chain was denoted as a weak intensity peak at 1107 cm^{-1}. Other absorption peaks at lower wavenumbers (780–600 cm^{-1}) may be ascribed to the variable-angle vibrations of COO^-. Based on these results, it can be concluded that $-CH_3$, $-CH_2$, COH, and C=O constitute the primary constituents of CPCMs.

Therefore, no new characteristic peaks were inferred, signifying that no chemical reaction occurred during the synthesis of CPCMs and that the adsorption of EG to eutectic PCM is incidental to physical effects rather than chemical ones. Overall, these observations established that the chemical properties of CPCMs correspond to those of fatty acids, demonstrating exceptional chemical stability. Such stability ensures that CPCMs retain their desired properties in asphalt pavement environments where consistent performance is crucial.

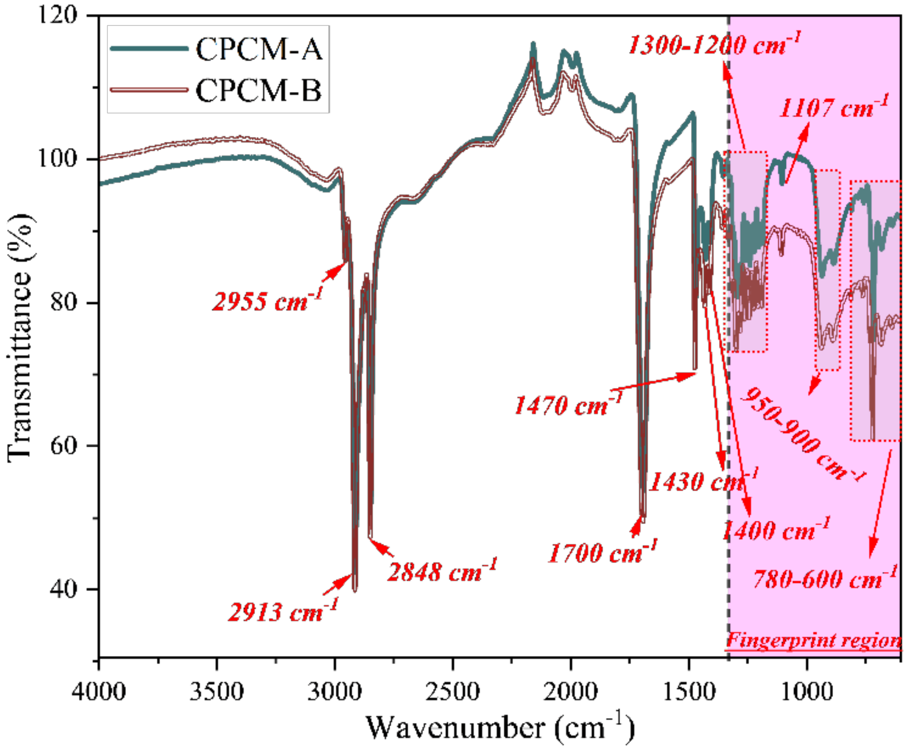

Figure 8 The FTIR spectrums of CPCMs

3.3.2 FTIR results of modified asphalt binders

The SBS, SBS-A, and SBS-B spectra are reported in Figure 9, underscoring the consistent molecular characteristics shared by these materials. The characteristic peaks resembling those of CPCMs were predominantly observed around 2900 cm^{-1}, 2850 cm^{-1}, 1470 cm^{-1}, and 1430 cm^{-1}. The peak at 1610 cm^{-1} in the three asphalt binders is attributed to the C=C stretching of the aromatic ring. In addition to the absorption peaks related to SBS-modified bitumen, fatty acid properties conveying absorption peaks were also evident, such as the characteristic peak at 1700 cm^{-1} and the characteristic peaks group within the range 1300-1200 cm^{-1} (falling within the fingerprint region), which were only discernible in the SBS-A and SBS-B spectra. These peaks are attributed to the carboxylic acid carbonyl C=O stretching and out-of-plane bending movements of the carboxylic acid C-OH. This spectral evidence indicated that CPCMs were seamlessly incorporated into the asphalt binder. Significantly, when comparing with SBS, no additional absorption peaks were observed apart from the characteristic peaks inherited from the CPCMs, indicating the chemical stability of composite phase change asphalt binders. Noticeable chemical stability is fundamental for realizing excellent thermal management performance for cooling asphalt pavement that employs PCM applications. This ensures that the material's intrinsic properties remain unchanged, fostering robust thermal management (Liu et al., 2020; Liu et al., 2021). These findings were further confirmed by Salman et al. (Hasanabadi et al., 2021) and Dong et al. (Zhang, D. et al., 2018), reinforcing the notion that incorporating CPCMs into binders without compromising their chemical stability offers a potential solution for improving the performance of asphalt pavements.

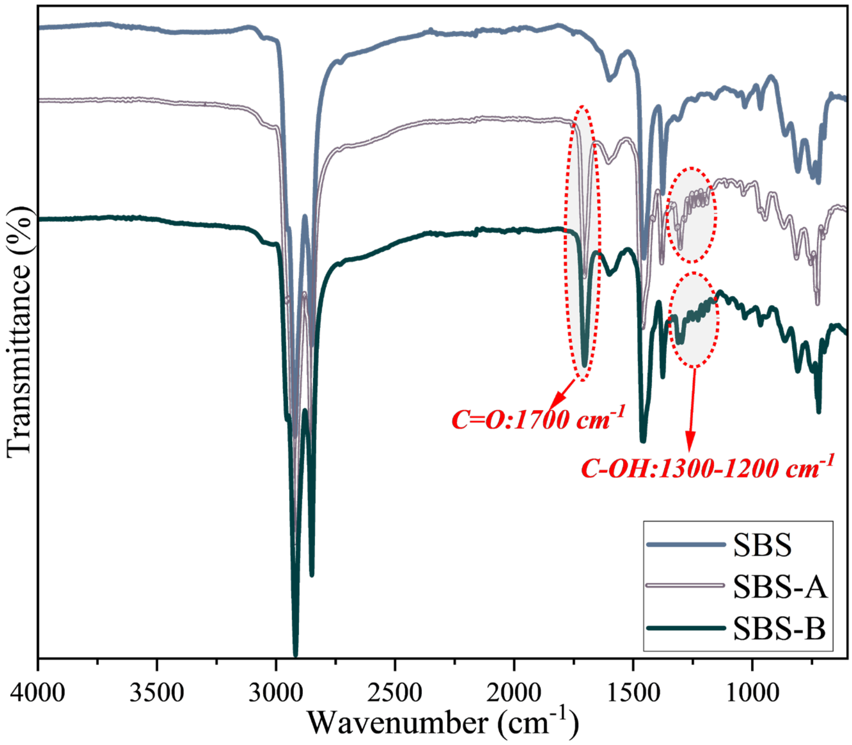

Figure 9 The FTIR spectrums of asphalt binders

3.4 Thermal stability of modified asphalt binders

An asphalt binder that demonstrates degradation or thermal decomposition at the production temperature of hot mix asphalt mixes (i.e. 180°C approx.) could significantly compromise the pavement's quality, longevity, and performance. As shown in Figure 10, SBS-A and SBS-B showed no thermal decomposition before 180°C, as their masses remained equal to 100%. This is a promising indicator for practical applications. Furthermore, the thermal decomposition of the asphalt binders proceeded through three distinct stages: a stable decomposition stage, a rapid decomposition stage, and an ultimate decomposition stage. The decomposition reaction of the original SBS-modified asphalt binder started at a temperature of 230°C and reached its maximum thermal decomposition rate at 466°C. The SBS-A and SBS-B displayed similar thermal decomposition trends, starting their thermal decomposition reactions at 190°C and their maximum thermal decomposition rates at 457°C and 461°C, respectively. Each of the three asphalt binders was decomposed at approximately 500°C, leaving a remaining mass of 77.1%, 79.4%, and 79.7%, respectively. These findings suggested that incorporating CPCMs into the SBS-modified asphalt binder decreased thermal stability, predominantly due to the thermal decomposition of CPCMs. This was evident through a faint peak between 200°C and 400°C in the derivative weight curves of SBS-A and SBS-B.

While CPCMs were responsible for reducing the thermal stability of asphalt binders, they maintained consistent mass up to 180°C, enabling SBS-modified asphalt binder with CPCMs to meet the thermal stability requirements for hot mix asphalt mixtures. Consequently, the benefits offered by CPCMs, such as enhanced temperature regulation, were achieved without detracting from the material's foundational requirements (Jin et al., 2019; Kheradmand et al., 2015).

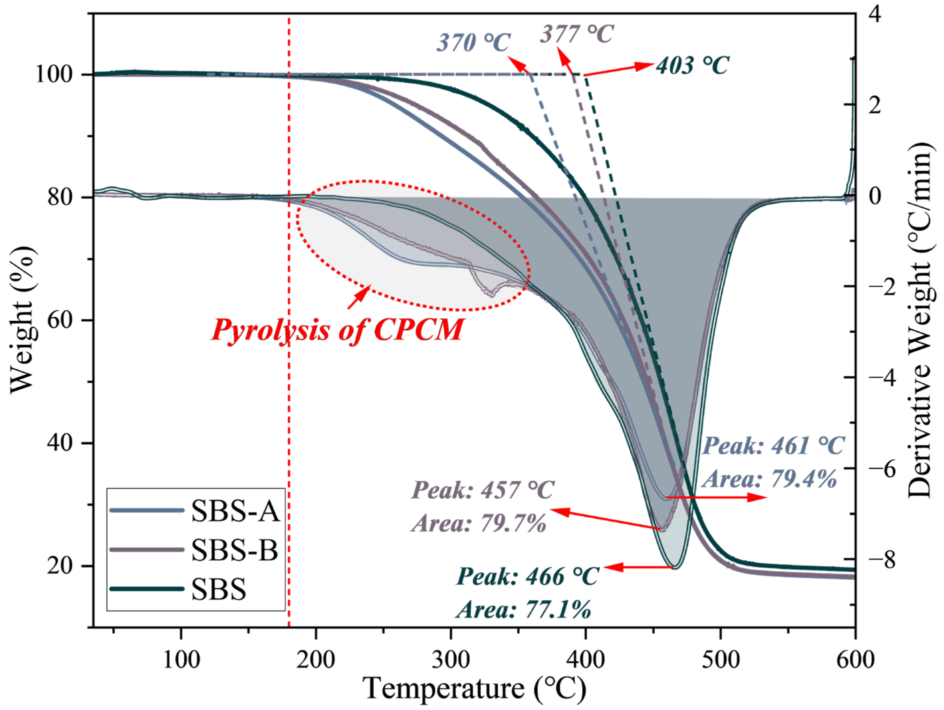

Figure 10 The TG and DTG curves of asphalt binders

3.5 Rheological performances of modified asphalt binders

3.5.1 Temperature sweep tests of modified asphalt binders

Figure 11 displays the results of the temperature sweep tests performed on the asphalt binders in the range of 20–70°C to identify the binder's thermal susceptibility. These parameters indicate the material's viscoelastic behavior and ability to withstand deformation (Jia et al., 2022). The phase angle of binders generally experiences a gradual increase while increasing temperature (Tarsi et al., 2020). The phase angle is a significant parameter that indicates the elastic proportion of a material. Specifically, it represents the tangent value of the storage and loss moduli. In an ideal scenario, the phase angle of an elastic body would be 0°, while that of a viscous body would be 90° (Zhang, H. et al., 2018). It is widely accepted that the asphalt binder undergoes a process of gradual softening with an increase in temperature, leading to a corresponding reduction in the relative elastic component. The phase angle of SBS-B was roughly 6° higher than that of both SBS and SBS-A before 40 ℃, and it remained higher throughout the whole temperature range of the test. This difference suggested that SBS-B was less elastic than the other two binders. Until 52°C, SBS-A had a phase angle comparable to SBS. As Figure 11 (a) indicates, the two distinct composite binders, SBS-B and SBS-A, had melting phase-change temperatures at 40 ℃ and 52 ℃, respectively, where an apparent change in the trend of δ-T curves could be observed. This indicates that the CPCM's phase-change temperature influenced the final binder's viscoelastic properties. To be specific, at the corresponding phase-change temperature, a distinct increase in the phase angle was observed: from 68.7° to 73.8° for SBS-B and from 67.7° to 71.7° for SBS-A. Interestingly, while the phase angle of SBS-B continues to increase with rising test temperature, SBS-A exhibited a reduction. Compared with the previous research, it is evident that the changes in the phase angle of SBS-A align with those of unencapsulated PCM asphalt composites, thereby confirming a small amount of leakage of CPCM. This may be due to the precipitation of PCM caused by the shear force during the preparation of the asphalt binders (Zhang, H. et al., 2018).

Moreover, as illustrated in Figure 11 (b), asphalt binders' complex shear modulus and rutting factors (G^*/Sin δ) gradually decreased, primarily due to the transition of binders from a highly elastic state to a more viscous flow state with increased temperature. Also noteworthy, the phase-change temperature of a CPCM was responsible for the sudden alteration of the complex shear modulus and rutting factor of the two composite binders. Before phase-change, SBS-A exhibited the highest complex modulus and rutting factor compared to the other two binders, indicating superior resistance to deformation. Conversely, SBS-B displayed the lowest deformation resistance. For instance, the complex modulus and rutting factor of SBS-A and SBS-B were approximately 3% higher and 5% lower than SBS at 28°C, respectively. This phenomenon is likely due to the premature phase-change of CPCMs in asphalt binders, which occurred earlier than 20°C owing to the mismatch in thermal conductivity between asphalt binder and CPCMs. Thereafter, SBS-A and SBS-B demonstrated comparable anti-deformation parameters roughly 20% lower than SBS after phase-change. The decline in resistance to deformation may be attributed to the minor leakage of CPCMs.

Overall, composite asphalt binders can experience enhanced deformation and temperature susceptibility resistance with higher phase-change temperature CPCMs such as SBS-A. It should be noted, however, that the leakage of CPCMs may result in reduced deformation resistance of the binder once its phase transformation has concluded. These findings are consistent with those of Zhang et al., (Zhang et al., 2019) and Jia et al., (Jia et al., 2022), demonstrating that incorporating CPCMs improves asphalt binders' temperature-dependent characteristics.

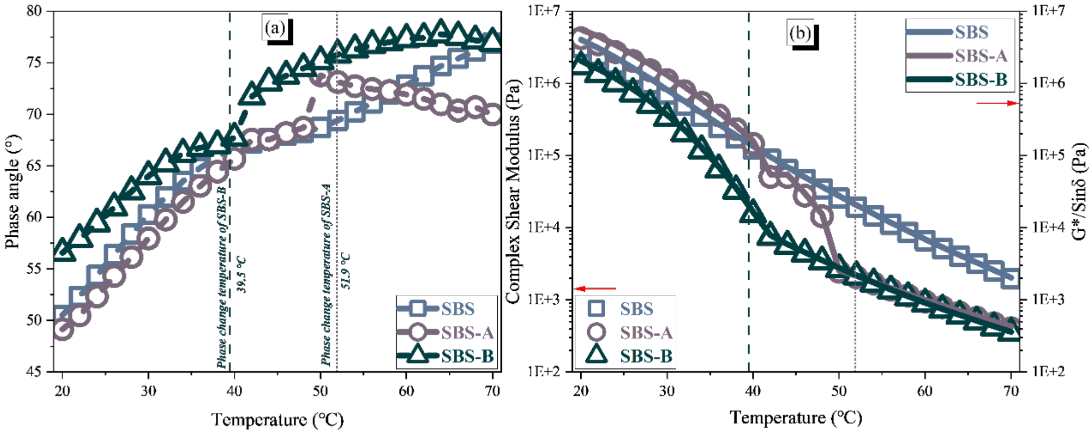

Figure 11 The temperature sweeps of asphalt binders: (a) phase angle, (b) complex shear modulus, and rutting factors

3.5.2 MSCR tests of modified asphalt binders

Figure 12 depicts the strain versus time curves of the performed MSCR tests, whereas Figure 13 is a radar chart showing the four crucial parameters (i.e., $R_{3.2}$, $R_{0.1}$, $J_{nr3.2}$, and $J_{nr0.1}$) at different test temperatures. The MSCR results demonstrated that the strain differential of binders as a function of time is affected by strain level and test temperature (Jia et al., 2021). Regardless of stress level, SBS-A and SBS-B exhibited higher accumulated strains than SBS at 30°C and 40°C. Notably, SBS-

B experienced the most significant strain accumulation among the three binders at both stress levels. For instance, the final accumulated strains of SBS-B, SBS-A, and SBS at 30°C and 0.1 kPa were 0.57%, 0.24%, and 0.22%, respectively. Thus, the SBS-B and SBS-A were 159.1% and 9.1% higher than the control SBS. At 3.2kPa, their final accumulated strains of SBS-A and SBS-B were were respectively 104% and 44.3% higher than those of SBS. These findings suggested that SBS-B may negatively impact the permanent deformation resistance of asphalt binder due to its more considerable cumulative strain. This reflects the more viscous-like behavior compared to SBS-A and SBS highlighted from the temperature sweep tests. As anticipated, this could be attributed to the faster phase change of CPCM-B. However, the strain curves showed a different trend at higher temperatures, namely 50°C and 60°C. The SBS exhibited a consistently higher cumulative strain than SBS-A and SBS-B, and the cumulative strain experienced at 0.1 kPa reached as high as 178.79% (at 50°C) and 767.78% (at 60°C). Similarly, these results supported the superior ability of SBS-A to resist high-temperature deformation than SBS and SBS-B.

Furthermore, to appraise the capacity of asphalt binders to endure long-term deformations under repeated loads at elevated temperatures, the average non-recoverable creep compliance at the two stress levels, known as J_{nr}, was utilized. Meanwhile, the elastic response of asphalt binders was assessed through the average percent recovery at different stress levels, represented by R (Saboo et al., 2018; Sun et al., 2019). As shown in Figure 13, the radar diagrams of MSCR parameters depicted the elastic response and non-recoverable creep compliance of the asphalt binders on the horizontal and vertical axes, respectively. It should be noted that lower J_{nr} denotes superior rutting resistance (Jia et al., 2021). Therefore, a tall vertical axis area and a decreased horizontal axis area indicate a remarkable ability for the asphalt binder to recover from creep deformation and vice versa.

Generally, at 30°C and 40°C, the MSCR radar charts for each of the three binders were ideal. As temperature rises, the radar map gradually evolves towards non-recoverable creep compliance. Nevertheless, the radar chart of SBS consistently demonstrated that using CPCMs may harm the recovery performance of asphalt binder, particularly under elevated temperatures and stress levels. Specifically, SBS-A exhibited $R_{0.1}$ values approximately 18% and 37% higher than SBS at 30°C and 40°C, respectively. Notably, SBS-A and SBS-B consistently displayed lower $R_{3.2}$ values and higher J_{nr} values than control SBS at elevated temperatures. The $R_{3.2}$ values of SBS-A and SBS-B were 15 times and 21 times lower than those of SBS, respectively, with the J_{nr} values being roughly 12 times higher than those of SBS (increasing from 0.8 1/kPa to 10 1/kPa).

To summarize, the SBS-A variant with a more significant phase transition temperature and lower leakage consistently demonstrated a lower susceptibility to stress and superior recovery capabilities than SBS-B.

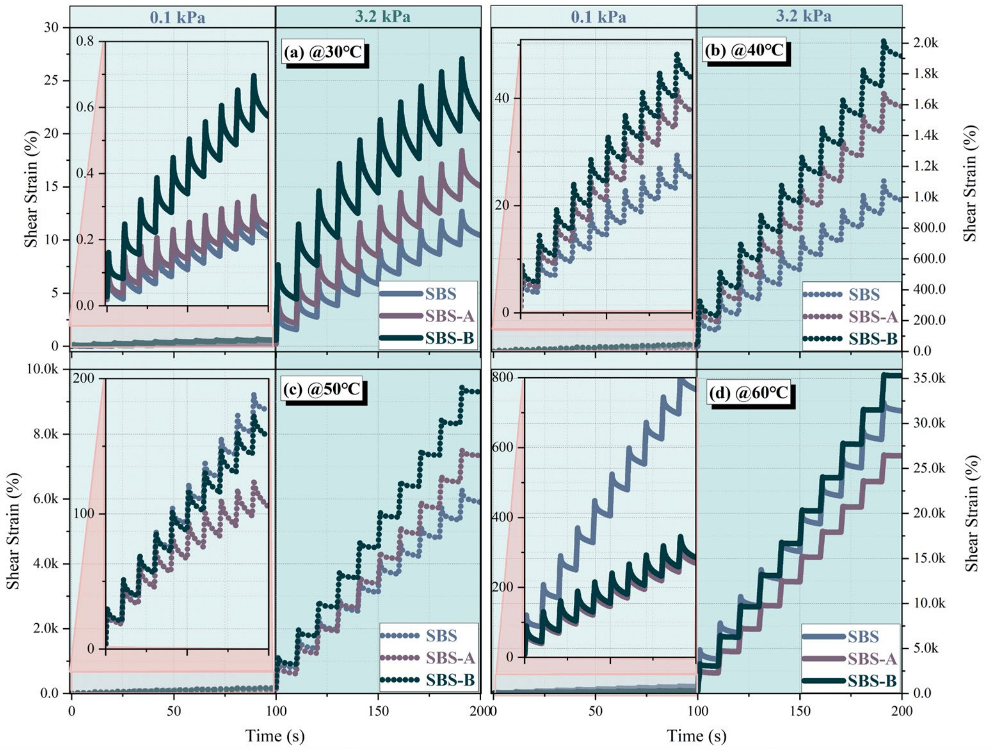

Figure 12 The shear strain of asphalt binders at different temperatures: (a) 30 °C, (b) 40 °C, (c) 50 °C, (d) 60 °C

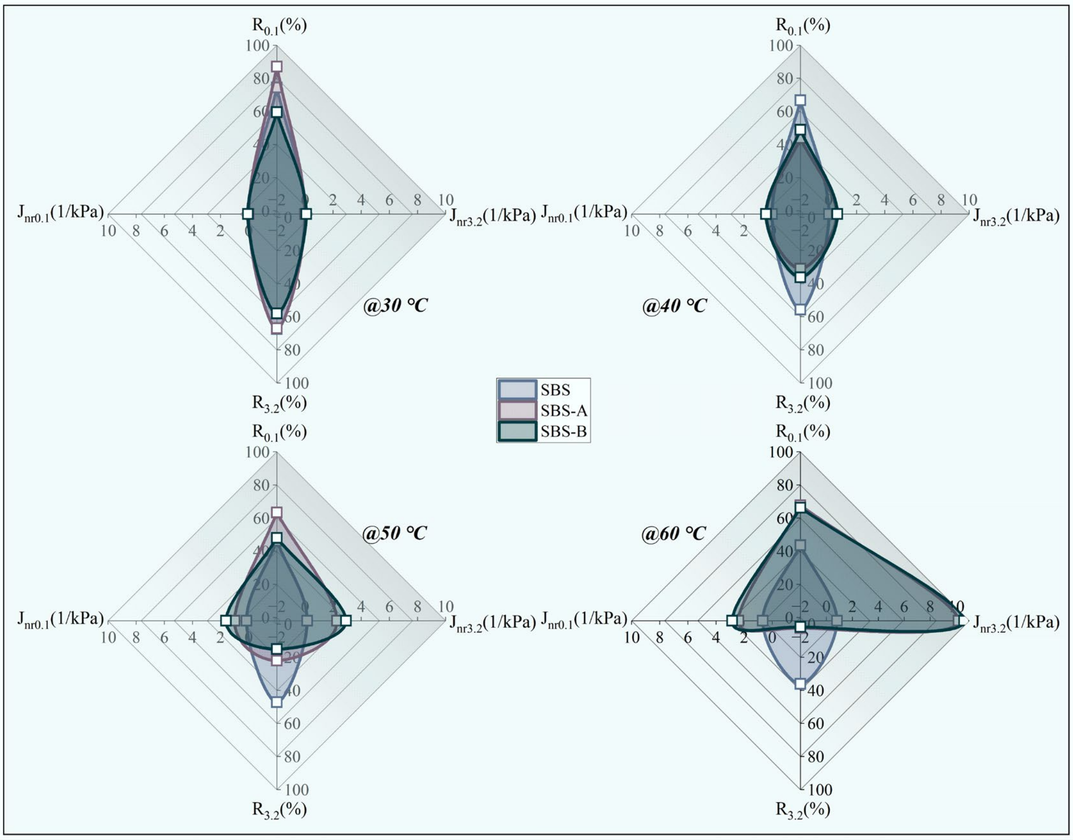

Figure 13 The MSCR parameters of asphalt binders

3.6 Thermal-regulating performance of modified asphalt binders

3.6.1 Phase change behaviors of modified asphalt binders

The heat flow curves of the three asphalt binder samples obtained from the DSC analysis are illustrated in Figure 14. The SBS did not exhibit the ability to carry latent heat, precluding the detection of any endothermic or exothermic peaks during its melting and crystallization processes. Thus, it does not possess temperature regulation capabilities. Conversely, SBS-A and SBS-B displayed notable endothermic and exothermic peaks in their respective heat flow curves, which indicated the successful integration of CPCMs. It means the asphalt binders' ability to carry latent heat. The melting enthalpy for SBS-A and SBS-B was 19.5 J/g and 17.2 J/g, respectively. Comparing their theoretical values of 29.4 J/g and 28.4 J/g, respectively, the calculated phase-change efficiency

E (that is, the measured value of melting enthalpy/the theoretical value of melting enthalpy) of SBS-A and SBS-B were approximately 66.3% and 61.6%, respectively. These phenomena could be attributed to the hindrance caused by the polymer crosslinking network structure of the SBS-modified asphalt binder towards the melting and crystallization of PCM. The endothermic and exothermic peaks of SBS-A and SBS-B exhibited a broader range of phase-change temperatures. However, the heat flow curves of asphalt binders differed from those of the corresponding CPCMs; in fact, their peaks were shifted leftward. Specifically, SBS-A demonstrated melting phase-change temperature and cooling phase-change temperature of 51.9°C and 28.2°C, respectively, which were lower than those of CPCMs-A by 9.8°C and 33.5°C. Similarly, the melting and cooling phase change temperatures of SBS-B were lower than those of CPCM-B, respectively, by 11°C and 28.7°C. Additionally, SBS-A and SBS-B exhibited supercooling effects of 23.7°C and 17.1°C, respectively. The decrease in phase-change temperature may be attributed to non-uniform thermal conductivity between the asphalt binders and CPCMs. Higher thermal conductivity in asphalt binders resulted in broader heat transfer, leading to an earlier phase-change reaction of CPCMs. Therefore, it is essential to consider the impact of asphalt binder on reducing phase-change temperature and enthalpy during PCM applications. The SBS-A had a higher cooling phase-change temperature than SBS-B, at 28.2° C and 22.4°C, respectively. The higher cooling phase-change temperature of SBS-A led the asphalt binder to be more suitable for the working environment of asphalt pavements, ensuring its phase-change cycle reaction in the corresponding working environment. Consequently, CPCMs endow SBS-modified asphalt binder with latent heat function to provide excellent temperature regulation performance. The CPCM-A may be the appropriate choice for cooling asphalt pavements compared to CPCM-B.

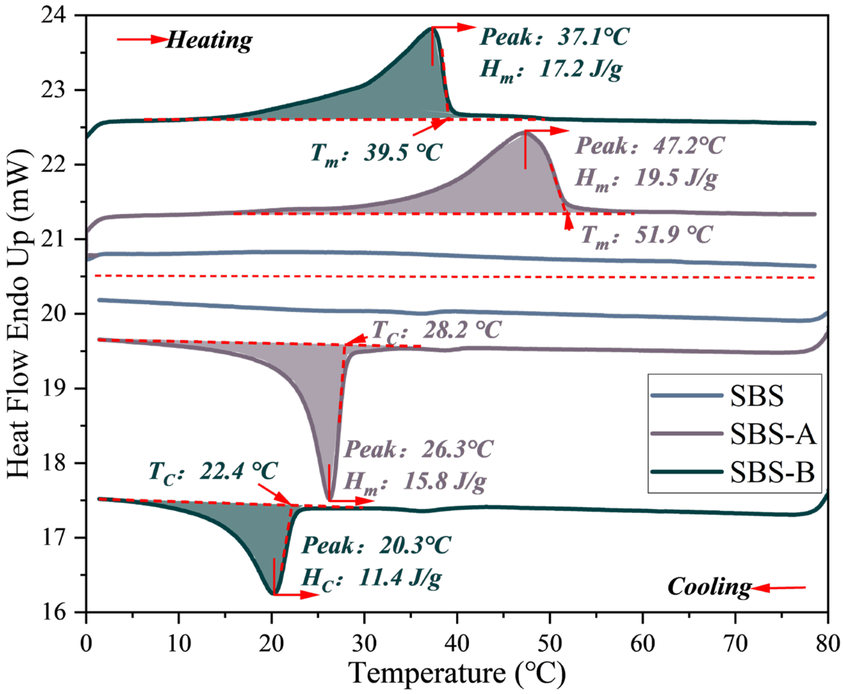

Figure 14 The heat flow curves of asphalt binders

3.6.2 Time-temperature curves of modified asphalt binders

Figure 15 presents the temperature-time curves of asphalt binders during heating and cooling periods. The regulating temperature ability of various CPCMs was analyzed by assessing the duration required for different modified asphalt materials to attain the same or different temperatures when subjected to identical heating and cooling times. It can be seen from Figure 15 (a) that the three asphalt binders exhibited discernible variations in their curve shapes. The temperature curve of SBS indicated a notable variance from SBS-A and SBS-B, with consistently higher temperature readings. The SBS-A and SBS-B reached 60°C at approximately 1440 seconds, while SBS was around 1770 seconds. The disparity between the control SBS and the other two composite binders indicated a temperature lag of 330 s. This finding highlights the increased susceptibility of SBS asphalt binder to thermal shock and temperature-related deterioration after adding CPCMs.

Moreover, it is worth noticing that a similar trend could be observed in the temperature curves of SBS-A and SBS-B, which displayed swift elevation from 8°C to 47°C within a timeframe of 600 s. As the heating continued, it was observed that the heating rate of SBS-B exhibited a gradual increase compared to SBS-A. For instance, the temperatures recorded for SBS, SBS-A, and SBS-B were 57°C, 55°C, and 53°C at 900 s. Additionally, the time required for each sample to reach 55°C was 750 s, 900 s, and 1080 s, respectively. These phenomena can be attributed to the fact that CPCMs endow the asphalt binder with latent heat properties. As a result, the binder accumulated heat in a latent form, considerably reducing its heating rate. The phase change temperature ranges of SBS-A and SBS-B were 10-40°C and 15-52°C, respectively. Once the phase change end temperature was surpassed, the heat was stored in the binder as sensible heat, accounting for the sudden rise in SBS-B beyond 40°C. Additionally, SBS-A consistently upheld the lowest heating rate, demonstrating excellent temperature adjustment ability, mainly due to the higher phase change enthalpy of CPCM-A (19.5 J/g) than that of CPCM-B (17.2 J/g). Various phase change temperatures and enthalpy of CPCMs affected the cooling process. During the cooling phase, these samples experienced a gradual decrease in temperature from 65°C to 8°C over 5600 s, 6060 s, and 6210 s, respectively. Notably, SBS demonstrated a slower cooling rate than SBS-A and SBS-B, taking an additional 610 s and 460 s, respectively, to reach an equilibrium temperature. The exothermic reaction in CPCMs can be considered responsible for these findings.

Specifically, as shown in Figure 15 (b), during the heating process of SBS-A and SBS-B, the maximum temperature difference of 13.1°C and 10.7°C was observed around 120 s and 150 s, respectively. Meanwhile, SBS-A and SBS-B exhibited temperature lags of 1500 s and 2610 s, respectively. Since the exothermic enthalpies of SBS-A and SBS-B were 3.7 J/g and 5.8 J/g lower than the endothermic enthalpies, respectively, the maximum temperature differences observed during the cooling process were 12.2°C and 6.5°C, respectively. Overall, incorporating CPCMs into asphalt binder provided their exceptional cooling capabilities through latent heat capacity. Nevertheless, SBS-A, which boasts higher phase change temperature and enthalpy, demonstrated a better ability to regulate temperature.

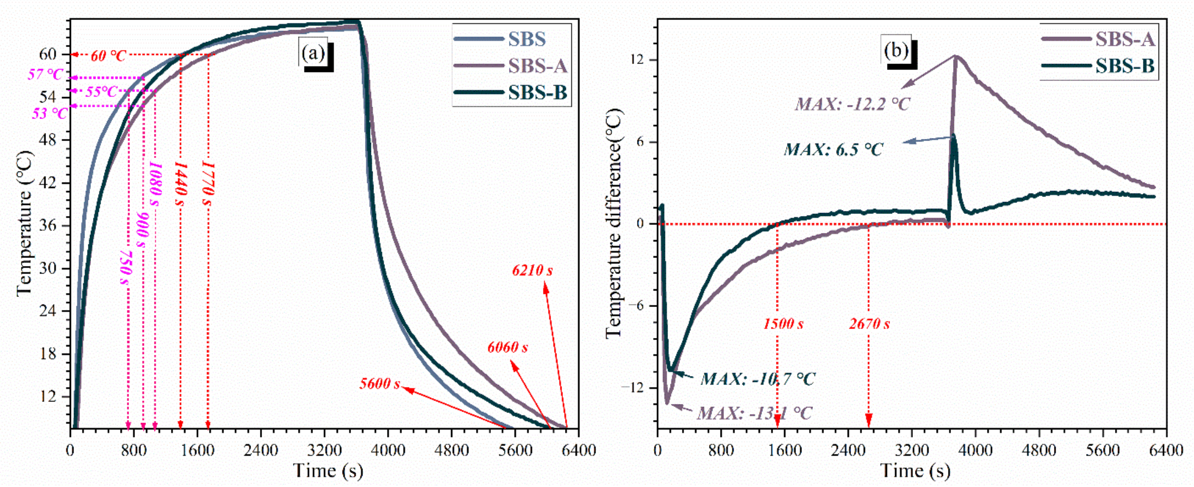

Figure 15 The temperature-time curves of asphalt binders

4. Conclusions

The primary goal of this study was to create two high-enthalpy CPCMs and integrate them into SBS-modified asphalt binders to explore their latent heat potential for cool asphalt pavements. Based on the findings, the following conclusions can be drawn:

(1) CPCM-A and CPCM-B demonstrated high adsorption efficiencies (over 90%) and substantial melting enthalpies. Their melting temperatures and thermal stability fit the asphalt pavement construction and service requirements.

(2) While CPCMs improved the rheological properties of the resulting binders, there was a need for a higher phase-change temperature. Compared to SBS-A, SBS-B underwent phase-change at an earlier stage, resulting in lower resistance to deformation. Meanwhile, CPCMs increased the

thermal and stress susceptibility of the asphalt binders, resulting in more significant strain accumulation, which may be detrimental.

(3) Incorporating CPCMs into SBS-modified asphalt increased its latent heat function, with notable heat storage and thermal-regulating capacity. Temperature differences of 13.1°C and 10.7°C were observed for SBS-A and SBS-B around 120 s and 150 s, respectively, with temperature lags of 1500 s and 2610 s, emphasizing their thermal behaviors.

(4) The infrared spectra analyses confirmed the chemical stability of both CPCMs and asphalt binders, indicating no chemical reactions during various processes. Although CPCMs marginally reduced the thermal stability of asphalt binders, the final product still met the thermal stability criteria for hot mix asphalt mixtures. CPCM-A emerged as a preferable choice for developing cool asphalt pavements among the studied materials.

While this work established the promising properties of CPCM-A and CPCM-B, further investigations on the encapsulation process of PCMs into the supporting materials and their long-term performances are necessary. Specifically, their durability and consistency should be assessed under continuous high temperatures, traffic loads, and various meteorological conditions in real-road environments. Conducting a thorough assessment of the uniform dispersion, thermal storage stability, and low-temperature flexibility displayed by PCMs when integrated into asphalt binders holds significant importance. Beyond performance evaluations, the potential of asphalt pavements using CPCMs in mitigating the UHI effect and other environmental benefits is pivotal.

5. Declaration of competing interest

The authors declared that they have no conflict of interest in this work.

6. Acknowledgments

Authors appreciate the funding support from the National Key R&D Program of China [grant number 2023YFBYFB2604600], the National Natural Science Foundation of China [grant number 52038001], the Fundamental Research Funds for the Central Universities, Chang'an University [grant number 300102213501 and CHD300102212704], and the China Scholarship Council [grant number 202106560029].

The authors would also like to express their gratitude to the Road Pavement Section of the University of Bologna for performing the experimental activities and for their valuable assistance in conducting all the tests.

References

Anderson, G.B., Bell, M.L., 2011. Heat waves in the United States: mortality risk during heat waves and effect modification by heat wave characteristics in 43 U.S. communities. Environ Health Perspect 119(2), 210-218.

Anupam, B.R., Sahoo, U.C., Rath, P., 2023. Effect of two organic phase change materials on the thermal performance of asphalt pavements. International Journal of Pavement Engineering 24(1).

ASTM, 2015. Standard Test Method for Multiple Stress Creep and Recovery (MSCR) of Asphalt Binder Using a Dynamic Shear Rheometer. ASTM, ASTM International, 100 Barr Harbor Drive, PO Box C700, West Conshohocken, PA 19428-2959. United States.

Bai, G., Fan, Q., Song, X.-M., 2018. Preparation and characterization of pavement materials with phase-change temperature modulation. Journal of Thermal Analysis and Calorimetry 136(6), 2327-2331.

Chen, J., Li, J., Wang, H., Huang, W., Sun, W., Xu, T., 2019. Preparation and effectiveness of composite phase change material for performance improvement of Open Graded Friction Course. Journal of Cleaner Production 214, 259-269.

Chen, Y., Wang, H., You, Z., Hossiney, N., 2020. Application of phase change material in asphalt mixture – A review. Construction and Building Materials 263.

Cheng, C., Cheng, G., Gong, F., Fu, Y., Qiao, J., 2021. Performance evaluation of asphalt mixture using polyethylene glycol polyacrylamide graft copolymer as solid–solid phase change materials. Construction and Building Materials 300.

Dai, J., Ma, F., Fu, Z., Li, C., Jia, M., Shi, K., Wen, Y., Wang, W., 2021. Applicability assessment of stearic acid/palmitic acid binary eutectic phase change material in cooling pavement. Renewable Energy 175, 748-759.

Dai, J., Ma, F., Fu, Z., Li, C., Wu, D., Shi, K., Dong, W., Wen, Y., Jia, M., 2022. Assessing the direct interaction of asphalt binder with stearic acid/palmitic acid binary eutectic phase change material. Construction and Building Materials 320.

Dai, J., Ma, F., Fu, Z., Liu, J., Li, C., Hou, Y., Wu, H., 2023. Effectiveness of the different eutectic phase-change materials in cooling asphalt pavement. Construction and Building Materials 407.

Du, W., Fei, H., He, Q., Wang, L., Pan, Y., Liu, J., 2021. Preparation and properties of capric acid-stearic acid-based ternary phase change materials. RSC Adv 11(40), 24938-24948.

Du, Y., Liu, P., Quan, X., Ma, C., Tian, J., Wu, X., 2021. Improving Rutting and Fatigue Properties of Asphalt Mastic by Adding Cement–Polyethylene Glycol Composite. Journal of Materials in Civil Engineering 33(10).

Du, Y., Liu, P., Wang, J., Wang, H., Hu, S., Tian, J., Li, Y., 2019. Laboratory investigation of phase change effect of polyethylene glycolon on asphalt binder and mixture performance. Construction and Building Materials 212, 1-9.

Farnam, Y., Krafcik, M., Liston, L., Washington, T., Erk, K., Tao, B., Weiss, J., 2016. Evaluating the use of phase change materials in concrete pavement to melt ice and snow. Journal of Materials in Civil Engineering 28(4), 04015161.

Gong, X., Liu, Q.T., Lv, Y., Chen, S.C., Wu, S.P., Ying, H., 2023. A systematic review on the strategies of reducing asphalt pavement temperature. Case Studies in Construction Materials 18.

Guo, M., Liang, M., Jiao, Y., Zhao, W., Duan, Y., Liu, H., 2020. A review of phase change materials in asphalt binder and asphalt mixture. Construction and Building Materials 258.

Haillot, D., Bauer, T., Kröner, U., Tamme, R., 2011. Thermal analysis of phase change materials in the temperature range 120–150°C. Thermochimica Acta 513(1-2), 49-59.

Hasanabadi, S., Sadrameli, S.M., Sami, S., 2021. Preparation, characterization and thermal properties of surface-modified expanded perlite/paraffin as a form-stable phase change composite in concrete. Journal of Thermal Analysis and Calorimetry 144(1), 61-69.

Hou, Y., Ma, F., Fu, Z., Li, C., An, Q., Zhu, C., Dai, J., 2023. Encapsulation of stearic-palmitic acid in alkali-activated coconut shell and corn cob biochar to optimize energy storage. Journal of Energy Storage 66.

Hu, H., Chen, W., Cai, X., Xu, T., Cui, H., Zhou, X., Chen, J., Huang, G., Sun, Y., 2021. Study on preparation and thermal performance improvements of composite phase change material for asphalt steel bridge deck. Construction and Building Materials 310.

Jia, M., Sha, A., Jiang, W., Wang, W., Li, J., Dai, J., Lu, Z., 2021. Laboratory evaluation of poly(ethylene glycol) for cooling of asphalt pavements. Construction and Building Materials 273.

Jia, M., Sha, A., Jiang, W., Wang, W., Yuan, D., 2023. Adhesion, rheology and temperature-adjusting performance of polyurethane-based solid–solid phase change asphalt mastics subjected to laboratory aging. Materials and Structures 56(3).

Jia, M., Sha, A., Jiang, W., Wang, W., Yuan, D., Li, J., Dai, J., Jiao, W., 2022. A solid–solid phase change filler with enhanced thermal properties for cooling asphalt mastic. Solar Energy 242, 105-118.

Jiao, W., Sha, A., Zhang, J., Jia, M., Jiang, W., Hu, L., 2023. Design and properties of polyurethane solid–solid phase-change granular temperature regulation asphalt mixtures. Solar Energy 253, 47-57.

Jin, J., Liu, L., Liu, R., Wei, H., Qian, G., Zheng, J., Xie, W., Lin, F., Xie, J., 2019. Preparation and thermal performance of binary fatty acid with diatomite as form-stable composite phase change material for cooling asphalt pavements. Construction and Building Materials 226, 616-624.

Jin, J., Liu, S., Gao, Y., Liu, R., Huang, W., Wang, L., Xiao, T., Lin, F., Xu, L., Zheng, J., 2021. Fabrication of cooling asphalt pavement by novel material and its thermodynamics model. Construction and Building Materials 272.

Jin, J., Xiao, T., Zheng, J., Liu, R., Qian, G., Xie, J., Wei, H., Zhang, J., Liu, H., 2018. Preparation and thermal properties of encapsulated ceramsite-supported phase change materials used in asphalt pavements. Construction and Building Materials 190, 235-245.

Kakar, M.R., Refaa, Z., Bueno, M., Worlitschek, J., Stamatiou, A., Partl, M.N., 2019a. Investigating bitumen's direct interaction with Tetradecane as potential phase change material for low temperature applications. Road Materials and Pavement Design 21(8), 2356-2363.

Kakar, M.R., Refaa, Z., Worlitschek, J., Stamatiou, A., Partl, M.N., Bueno, M., 2019b. Effects of aging on asphalt binders modified with microencapsulated phase change material. Composites Part B: Engineering 173.

Ke, H., 2017. Phase diagrams, eutectic mass ratios and thermal energy storage properties of multiple fatty acid eutectics as novel solid-liquid phase change materials for storage and retrieval of thermal energy. Applied Thermal Engineering 113, 1319-1331.

Kheradmand, M., Castro-Gomes, J., Azenha, M., Silva, P.D., de Aguiar, J.L.B., Zoorob, S.E., 2015. Assessing the feasibility of impregnating phase change materials in lightweight aggregate for development of thermal energy storage systems. Construction and Building Materials 89, 48-59.

Kolyado, A.V., Alenova, S.M., Garkushin, I.K., 2016. Phase diagram of a system of adipic, glutaric, and sebacic acids. Russian Journal of Physical Chemistry A 90(6), 1293-1297.

Li, C., Zhang, B., Xie, B., Zhao, X., Chen, J., Chen, Z., Long, Y., 2019. Stearic acid/expanded graphite as a composite phase change thermal energy storage material for tankless solar water heater. Sustainable Cities and Society 44, 458-464.

Li, H., Harvey, J., Jones, D., 2013. Cooling Effect of Permeable Asphalt Pavement under Dry and Wet Conditions. Transportation Research Record 2372(1), 97-107.

Liu, C., Yuan, Y.P., Zhang, N., Cao, X.L., Yang, X.J., 2014. A novel PCM of lauric-myristic-stearic acid/expanded graphite composite for thermal energy storage. Materials Letters 120, 43-46.

Liu, Q., Wu, L., Wang, Y., Tang, N., Wang, X., Gao, L., Wang, Q., 2022. A novel functional coating with 2DMts/SA phase change material as filler and its pavement temperature regulation performance. Materials Letters 306.

Liu, T., Guo, N., Jin, X., Tan, Y., You, Z., Cui, S., Chu, Z., Fang, C., 2023. Thermoregulation, rheological properties and modification mechanism of asphalt modified with PUSSPCMs. Construction and Building Materials 372.

Liu, Z., Wang, Y., Jia, J., Sun, H., Wang, H., Qiao, H., 2020. Preparation and Characterization of Temperature-Adjusting Asphalt with Diatomite-Supported PEG as an Additive. Journal of Materials in Civil Engineering 32(3).

Liu, Z., Wei, K., Wang, S., Ma, B., Wang, X., Shi, W., Xu, J., 2021. Effect of high-temperature-resistant epoxy resin/polyethylene glycol 2000 composite stereotyped phase change material particles on asphalt properties. Construction and Building Materials 300.

Ma, B., Wang, X.-q., Zhou, X.-y., Wei, K., Huang, W., 2019. Measurement and analysis of thermophysical parameters of the epoxy resin composites shape-stabilized phase change material. Construction and Building Materials 223, 368-376.

Ma, G., Sun, J., Xie, S., Wang, Z., Jing, Y., Jia, Y., 2018. Solid-liquid phase equilibria of stearic acid and dicarboxylic acids binary mixtures as low temperature thermal energy storage materials. The Journal of Chemical Thermodynamics 120, 60-71.

Ma, Y., Yang, H., Zuo, H., Zuo, Q., He, X., Chen, W., Wei, R., 2023. EG@Bi-MOF derived porous carbon/lauric acid composite phase change materials for thermal management of batteries. Energy 272.

Nazir, H., Batool, M., Ali, M., Kannan, A.M., 2018. Fatty acids based eutectic phase change system for thermal energy storage applications. Applied Thermal Engineering 142, 466-475.

Nwakaire, C.M., Onn, C.C., Yap, S.P., Yuen, C.W., Onodagu, P.D., 2020. Urban Heat Island Studies with emphasis on urban pavements: A review. Sustainable Cities and Society 63.

Roman, K.K., O'Brien, T., Alvey, J.B., Woo, O., 2016. Simulating the effects of cool roof and PCM (phase change materials) based roof to mitigate UHI (urban heat island) in prominent US cities. ENERGY 96, 103-117.

Saboo, N., Kumar, R., Kumar, P., Gupta, A., 2018. Ranking the Rheological Response of SBS- and EVA-Modified Bitumen Using MSCR and LAS Tests. Journal of Materials in Civil Engineering 30(8).

Salem, T., Bichara, L., 2023. Mitigation of UHI Effect with the Incorporation of PCM in Concrete Pavement-Case Study: City of Rotterdam.

Seki, Y., İnce, Ş., Ezan, M.A., Turgut, A., Erek, A., 2015. Graphite nanoplates loading into eutectic mixture of Adipic acid and Sebacic acid as phase change material. Solar Energy Materials and Solar Cells 140, 457-463.

Sun, Y., Wang, W., Chen, J., 2019. Investigating impacts of warm-mix asphalt technologies and high reclaimed asphalt pavement binder content on rutting and fatigue performance of asphalt binder through MSCR and LAS tests. Journal of Cleaner Production 219, 879-893.

Tarsi, G., Caputo, P., Porto, M., Sangiorgi, C., 2020. A Study of Rubber-REOB Extender to Produce Sustainable Modified Bitumens. Applied Sciences 10(4).

Tyagi, V.V., Chopra, K., Kalidasan, B., Chauhan, A., Stritih, U., Anand, S., Pandey, A.K., Sari, A., Kothari, R., 2021. Phase change material based advance solar thermal energy storage systems for building heating and cooling applications: A prospective research approach. Sustain Energy Techn 47.

Wang, C., Wang, Z.-H., Kaloush, K.E., Shacat, J., 2021. Cool pavements for urban heat island mitigation: A synthetic review. Renewable and Sustainable Energy Reviews 146.

Wang, H., Wang, Y., Qi, M., Wang, Q., Li, X., Zhu, X., Yu, X., Liu, Z., 2021. PEG/diatomite modified Asphalt Mixture with Self-Regulating temperature property. Case Studies in Construction Materials 15.

Wei, K., Liu, Z., Wang, L., Ma, B., Fan, Y., Shi, J., Cheng, P., 2022. Preparation of polyurethane solid-solid low temperature PCMs granular asphalt mixes and study of phase change temperature control behavior. Solar Energy 231, 149-157.

Wu, L., Liu, Q., Tang, N., Wang, X., Gao, L., Wang, Q., Lv, G., Hu, L., 2022. Development of two-dimensional nano Mts/SA phase change materials for self-adjusting temperature of pavement. Construction and Building Materials 349.

Yang, L., Cao, X., Zhang, N., Xiang, B., Zhang, Z., Qian, B., 2019. Thermal reliability of typical fatty acids as phase change materials based on 10,000 accelerated thermal cycles. Sustainable Cities and Society 46.

Ye, H., Long, L., Zhang, H., Zou, R., 2014. The performance evaluation of shape-stabilized phase change materials in building applications using energy saving index. Applied Energy 113, 1118-1126.

Yinfei, D., Pusheng, L., Jiacheng, W., Hancheng, D., Hao, W., Yingtao, L., 2020. Effect of lightweight aggregate gradation on latent heat storage capacity of asphalt mixture for cooling asphalt pavement. Construction and Building Materials 250.

Yuan, D., Jiang, W., Sha, A., Xiao, J., Wu, W., Wang, T., 2023a. Technology method and functional characteristics of road thermoelectric generator system based on Seebeck effect. Applied Energy 331.

Yuan, D., Jiang, W., Xiao, J., Ling, X., Zhang, Y., Lu, R., 2023b. Experimental study on the temperature-regulating function of road thermoelectric generator system. Journal of Cleaner Production 384.

Zhang, D., Chen, M., Wu, S., Liu, P., 2021. Effect of expanded graphite/polyethylene glycol composite phase change material (EP-CPCM) on thermal and pavement performance of asphalt mixture. Construction and Building Materials 277.

Zhang, D., Chen, M., Wu, S., Liu, Q., Wan, J., 2018. Preparation of expanded graphite/polyethylene glycol composite phase change material for thermoregulation of asphalt binder. Construction and Building Materials 169, 513-521.

Zhang, D., Chen, M.Z., Wu, S.P., Riara, M., Wan, J.M., Li, Y.Y., 2019. Thermal and rheological performance of asphalt binders modified with expanded graphite/polyethylene glycol composite phase change material (EP-CPCM). Construction and Building Materials 194, 83-91.

Zhang, D.R., Sani, B.M., Xu, P.X., Liu, K., Gu, F., 2023. Preparation and characterization of binary eutectic phase change material laden with thermal conductivity enhancer for cooling steel slag asphalt pavement. Construction and Building Materials 388.

Zhang, H., Chen, Z., Xu, G., Shi, C., 2018. Evaluation of aging behaviors of asphalt binders through different rheological indices. Fuel 221, 78-88.

Zhang, J., Dong, Z., Sun, G., Qi, Y., Zhu, X., Li, Y., 2023. Roles of phase change materials on the morphological, physical, rheological and temperature regulating performances of high-viscosity modified asphalt. Sci Total Environ 875, 162632.